Supplemental Material

Isolation of human CPCs

Approximately 20-50 mg of right atrial (RA) appendage tissue routinely removed during surgical repair of congenital heart defects was collected for cell isolation. Tissue samples were transported from the Children's Healthcare of Atlanta at Egleston Hospital to the laboratory in Krebs-Ringer solution (35 mmol/L NaCl, 4.75 mmol/L KCl, 1.2 mmol/L KH2PO4, 16 mmol/L Na2HPO4, 135 mmol/L sucrose, 25 mmol/L NaHCO3, 10 mmol/L glucose, 10 mmol/L HEPES, and 30 mmol/L 2,3-butanedione monoxime, pH 7.4 with NaOH). CPCs were isolated within 4 hours of sample acquisition by magnetic bead sorting for c-Kit protein as described previously [9]. Samples were collected from 32 individual patients of 3 different age groups (9 neonates, 15 infants, and 8 children).

RNAseq

RNA-seq analysis was conducted at the Yerkes Nonhuman Primate Genomics Core Laboratory. RNA was purified from confluent hCPCs using Trizol per manufacturer's protocol, and RNA quality was assessed using an Agilent Bioanalyzer. Libraries were prepared using the Illumina TruSeq™ mRNA stranded kit (Illumina Inc. San Diego, CA, USA) as per manufacturer's instructions. 1000 ng of total RNA was used for library preparation. ERCC (Ambion) synthetic spike-in 1 or 2 was added to each Total RNA sample and processed in parallel. The TruSeq method (high-throughput protocol) employs two rounds of poly-A based mRNA enrichment using oligo-dT magnetic beads followed by mRNA fragmentation (120-200 bp) using cations at high temperature. First and second strand cDNA synthesis was performed followed by end repair of the blunt cDNA ends and ligation of the adapters. The adapter-ligated libraries were then enriched using PCR amplification. The amplified library was validated using a DNA tape on the Agilent 4200 TapeStation and quantified using a fluorescence based method. The libraries were normalized and pooled, clustered on an Illumina cBot, and then sequenced on the Illumina HiSeq3000 system employing a single-end 101 cycle flow cell. The average read depth for the samples was 22,568,201 reads. Following de-identification of individual patients, all data were deposited in the GEO database (GSE126251).

CPC and MSC culture

Human CPCs were cultured in Ham's F12 medium supplemented with 10% fetal bovine serum (FBS), 100 U/mL penicillin/streptomycin, 2 mmol/L L-glutamine, and 0.01 µg/mL basic fibroblast growth factor (bFGF). CPC conditioned media was produced by culturing confluent CPCs in media devoid of FBS and bFGF for 12 hours after first quiescing cells in media devoid of FBS and bFGF for 8 hours. MSCs were cultured in growth media containing MEM base media (Minimum Essential Medium Eagle's) supplemented with 10% FBS, 1% antibiotic-antimycotic, and 1% L-glutamine. Quiescing media for both cell types contains growth media minus serum (and FGF2 for hCPCs).

Proliferation assay

Proliferation was measured using a Click-it EdU Microplate Assay (Invitrogen; Catalog no. C10214). Neonatal c-kit+ progenitor cells (CPCs) with growth media were plated at 10,000 cells per well in 96 well plates and incubated at 37°C overnight. After 24 hours, 5-Ethynyl-29-deoxyuridine (EdU) reagent was added and cells were incubated for an additional 24 hours. The

cells were then fixed and reacted with Oregon Green 488 per manufacturer's protocol. Anti-Oregon Green antibody conjugated with horseradish peroxidase was then added followed by the addition of Amplex Ultra Red substrate to produce a red fluorescent product. The absorbance of the samples was read with a BioTek Synergy 2 plate reader at 530/590 nm. In each experiment, the absorbance of each cell line was normalized by the maximum signal in that same experiment. Proliferation assay was performed N=5 times for each cell line. For an unbiased analysis, same passage number was used for each cell line at each experiment. We used different passages for different technical replicates.

Migration assay

Migration was determined using the modified Boyden chamber method. One hundred thousand MSCs were seeded in the top well of Boyden chamber (Corning; catalog no. 3422) and allowed to adhere to and migrate through the membrane. The cells were quiesced with serum free media for 24 hours while conditioned media was added to the lower chamber (assay was performed in duplicate). Conditioned media was obtained from different passages of neonatal CPCs which were quiesced for 24 hours. After 24 hours of incubation, migrated cells were detached from the bottom part of the membrane using cell dissociation solution (Trevigen; catalog no. 3455-096-05) and labeled with tracker Orange CMRA (Life Technologies; catalog no. C34551). After 1-hour incubation, cell migration was quantified by measuring CMRA fluorescence on a plate reader (BioTek Synergy 2) at 530/590 nm. The absorbance of each sample was normalized by the maximum signal quantified in the same experiment. Migration assay was done N=5 for each cell line.

ELISA assay

Conditioned media from different passages of quiesced neonatal CPCs were collected after 24 hours of incubation. The level of secreted proteins of interest (IL-1α, IL-1β, IL-24, CXCL6, CXCL8) were quantified by specific ELISA kits (RayBiotech; Catalog no. ELH-IL1a, ELH-IL1b, ELH-IL24, ELH-GCP2, ELH-IL8 respectively). All immunosorbent measures were normalized to the maximum protein signal. ELISA was performed N=3 for each cell line.

Statistical modeling and pathway analysis

Principal component (PC) analysis and partial least squares regression (PLSR) analysis were performed using SIMCA-P software (UMetrics, now part of Sartorius Stedim Biotech; https://umetrics.com) that solves the PLSR problem with the nonlinear partial least squares algorithm. RNA-seq analyses were performed by aligning (paired) end reads to the reference human genome (*Homo sapiens* (PAR-masked)/hg 19) with TopHat and read depth at the level of individual genes was computed with Cufflinks on the Illumina BaseSpace. These raw intensity values were converted to counts per million, log2 transformed, and normalized by several strategies to control for possible hidden sources of variability. Specifically, mRNA data between patients were normalized either to the maximum signal for each gene, or mean-centered across the full distribution of read counts. Results obtained from each normalization method were comparable, and those obtained with the mean centering are presented in Figures and discussed in the paper.

Two-way hierarchical clustering analysis of standard normalized gene expression (z-scores) for selected genes was performed using Ward's method (JMP v13, SAS Institute, Cary, NC). Volcano plots were drawn by plotting significance (-log p-value) against difference in abundance (log 2 scale) of the genes between good and poor c-kit+ progenitor cells. Correlation of highly differentiated genes with proliferation and migration cardiac responses was analyzed with JMP statistical software, fitting Y (responses) against X (gene expression level). For

pathway analysis of gene clustering, we used Ingenuity Pathway Analysis (IPA) software. RNA expression level data were analyzed for enrichment of specific biological functions using IPA. Statistical analysis was performed using GraphPad Prism software. One-way ANOVA was used with Tukey's post-test for the comparison of multiple groups. P-values of less than 0.05 were considered significant. Data are represented as mean ± standard error of the mean (SEM). Average accuracy between observed and predicted responses was measured by calculating the average differences between observed and predicted response among all samples. Predictability of the models was defined by calculating the R square values of regression models.

Supplementary Table 1. List of highly correlated genes with both proliferation and migration (91 genes).

Top genes correlated with proliferation and migration	Top genes correlated with proliferation and migration	Top genes correlated with proliferation and migration	Top genes correlated with proliferation and migration
ABHD17C	HDGF	MME	SLC11A2
AGTRAP	HHEX	MOB3B	SLC1A3
ATG7	HIF3A	NFKB1	SLC35D2
B3GNT5	HPSE	NFKB2	SLC44A5
BCL2	IL1A	NFKBIA	SMOX
BCL6B	IL1B	NFKBIE	SOD2
BTF3	ISOC1	NOTCH4	TGIF1
C11orf84	KCNK1	NRCAM	TIE1
CACNB3	KHNYN	PDE4D	TMCC3
CHMP1B	KIAA1804	PHACTR1	TMEM132A
CUL1	KIFC3	PIK3CD	TMEM170A
CXCL1	KLF3	POU2F2	TMEM205
CXCL6	KLHL17	PRKD2	TMEM39B
CXCL8	LIMD2	PTGS2	TNIP1
DCLK3	LINC00473	PTPN9	TOP1MT
EGFL7	LINC01137	RAB3D	TRIM24
EIF3D	LMBR1L	RELB	TRIM8
ERO1B	LOC100505622	RPL4	UBALD2
FLI1	LOC101928100	RPS3	UCKL1
FMNL2	LRRC15	RPS7	VPS37C
FTH1	MED30	S1PR1	WTAP
GIPC3	MEN1	SEMA4C	ZC3H12A
GPR153	MLLT4	SH3BP1	

Supplementary Table 2. List of GOOD and POOR-quality c-kit+ progenitor cell lines.

Patient	Quality	Patient	Quality
Neonate 903	GOOD	Infant 957	POOR
Neonate 925	GOOD	Infant 975	POOR
Neonate 930	GOOD	Infant 1054	POOR
Neonate 1045	GOOD	Infant 1089	POOR
Neonate 1050	GOOD	Infant 1094	POOR
Neonate 1059	GOOD	Infant 1096	POOR
Neonate 1075	GOOD	Infant 1097	POOR
Neonate 1082	GOOD	Infant 1099	POOR
Neonate 1083	GOOD	Child 1063	GOOD
Infant 924	GOOD	Child 1065	GOOD
Infant 985	GOOD	Child 902	POOR
Infant 998	GOOD	Child 926	POOR
Infant 1057	GOOD	Child 938	POOR
Infant 1066	GOOD	Child 940	POOR
Infant 896	POOR	Child 1048	POOR
Infant 956	POOR	Child 1092	POOR

Supplementary Table 3. List of genes upregulated at least 2-fold or are significantly increased (p<10-4) in GOOD vs POOR c-kit+ progenitor cells.

At least 4-fold upregulated genes in Good vs Poor patients	At least 4-fold upregulated genes in Good vs Poor patients	Significantly increased genes in Good vs Poor patients	Significantly increased genes or genes upregulated at least 4-fold in Good vs Poor patients	Significantly increased genes or genes upregulated at least 4-fold in Good vs Poor patients	Significantly increased genes or genes upregulated at least 4-fold in Good vs Poor patients
C3	IL1B	IGF2BP2	C3	IL1A	S1PR1
CADPS2	IL24	KIAA1804	CADPS2	IL1B	SLC35D2
CARD11	IRAK3	MICB	CARD11	IL24	SLC6A15
CSF2	KCNK1	PTBP1	CSF2	IRAK3	SLC7A2
CXCL1	KIAA1804	RBM10	CXCL1	KCNK1	STARD10
CXCL2	LAMP3	RPL14	CXCL2	KIAA1804	STRN4
CXCL6	LOC100505622	SLC35D2	CXCL6	LAMP3	TFPI2
CXCL8	MDFI	STARD10	CXCL8	LOC100505622	TIE1
DSC2	MME	STRN4	DSC2	MDFI	
EPB41L3	NRCAM		EPB41L3	MICB	
FAM163A	PDZK1IP1		FAM163A	MME	
FBN2	POU2F2		FBN2	NRCAM	
GPR4	S1PR1		GPR4	PDZK1IP1	
HIF3A	SLC6A15		HIF3A	POU2F2	
HPSE	SLC7A2		HPSE	PTBP1	
HSD11B1	TFPI2		HSD11B1	RBM10	
IL1A	TIE1		IGF2BP2	RPL14	

Supplementary Table 4. List of canonical signaling pathways of highly differentiated genes (42 genes) that are associated with cardiac and immune responses.

Canonical Pathways	-log (p-value)
Granulocyte Adhesion and Diapedesis (Inflammatory Response)	8.17
Agranulocyte Adhesion and Diapedesis (Macrophage, Lymphocyte, Monocyte)	6.72
Role of Cytokines in Mediating Communication between Immune Cells (Immune Response)	5.98
IL-8 Signaling (Innate Immunity)	5.17
Cytokine Production in Macrophages and T Helper (Immune Response)	4.49
TREM1 Signaling (Inflammatory Response)	3.97
HMGB1 Signaling (Transcriptional Regulation)	3.92
Communication between Innate and Adaptive Immune Cells (Immune Response)	3.61
Complement System (Immune Response)	3.57
Fcγ Receptor-mediated Phagocytosis in Macrophages and Monocytes (Immune Response)	3.5
Hematopoiesis from Pluripotent Stem Cells (Blood Cell Formation)	3.37
STAT3 Pathway (Cellular Growth and Apoptosis, Immune Response Factor)	3.33
LXR/RXR Activation (Transcription Factor)	3.06
Integrin Signaling (Cell Adhesion, Migration, Immune Response)	3.05
Atherosclerosis Signaling	3.02
Natural Killer Cell Signaling (Immune Response)	3
Glucocorticoid Receptor Signaling (Immune Response Regulator, Fetal Heart Development)	2.9
Netrin Signaling (Angiogenesis)	2.81
Agrin Interactions at Neuromuscular Junction (Cardiac Cell Regeneration)	2.67

Ephrin B Signaling	2.67
Toll-like Receptor Signaling	2.63
IL-15 Signaling (Immune Response)	2.52
Acute Phase Response Signaling (Immune Response)	2.48
Ephrin Receptor Signaling	2.46
Toll-like Receptor Signaling	2.63
IL-15 Signaling (Immune Response)	2.52
Acute Phase Response Signaling (Immune Response)	2.48
Ephrin Receptor Signaling	2.46
NF-κB Signaling	2.4
ERK/MAPK Signaling (Cell Cycle and Proliferation)	2.25
Leukocyte Extravasation Signaling (Immune Response)	2.23
SAPK/JNK Signaling (Proliferation, Apoptosis)	2.18
p38 MAPK Signaling (Immune Response)	2.06
PTEN Signaling (Cell Proliferation)	2.02
IL-6 Signaling (Immune Response)	1.93
Neuroinflammation Signaling Pathway	1.67
IL-10 Signaling (Immune Response)	1.61
MSP-RON Signaling Pathway (macrophage activity, wound healing)	1.58
Dendritic Cell Maturation (Immune Response)	1.57
B Cell Receptor Signaling (Immune Response)	1.54
GM-CSF Signaling (Immune Response)	1.5
Regulation of IL-2 Expression in Activated and Anergic T Lymphocytes (Immune Response)	1.45
IL-3 Signaling (Immune Response)	1.41

Crosstalk between Dendritic Cells and Natural Killer Cells (Immune Response)	1.41
IL-17 Signaling (Immune Response)	1.39
Hematopoiesis from Multipotent Stem Cells (Regeneration)	1.38
IL-1 Signaling (Immune Response)	1.38
PRAR Signaling (Proliferation)	1.33

Supplementary Table 5. Canonical pathway analysis. Ingenuity pathways analysis (IPA) was used to determine top canonical pathways for the overlapping genes between original top 300 genes and the 42 highly differentiated genes. Pathway analysis demonstrated that these genes are involved in pathways such as cardiovascular system development and function, immune response pathways and networks, and cellular growth and proliferation. The two sets of genes share several same canonical pathways.

Canonical Pathways	-log (p-value)
Granulocyte Adhesion and Diapedesis	7.47
Agranulocyte Adhesion and Diapedesis	5.91
IL-8 Signaling	4.33
Complement System	4.31
Integrin Signaling	4.23
LXR/RXR Activation	4.02
FXR/RXR Activation	3.97
Natural Killer Cell Signaling	3.96
Netrin Signaling	3.54
Role of IL-17A in Arthritis	3.46
Acute Phase Response Signaling	3.41
Agrin Interactions at Neuromuscular Junction	3.39
Ephrin B Signaling	3.39
Ephrin Receptor Signaling	3.39

Differential Regulation of Cytokine Production in Macrophages and T Helper Cells by IL-17A and IL-17F	3.24
Regulation of Actin-based Motility by Rho	3.18
ERK/MAPK Signaling	3.17
Fcγ Receptor-mediated Phagocytosis in Macrophages and Monocytes	3.08
STAT3 Pathway	2.96
SAPK/JNK Signaling	2.88
Atherosclerosis Signaling	2.72
Fc Epsilon RI Signaling	2.71
PTEN Signaling	2.71
HMGB1 Signaling	2.6
PKCθ Signaling in T Lymphocytes	2.41
Glucocorticoid Receptor Signaling	2.34
Role of Cytokines in Mediating Communication between Immune Cells	2.32
B Cell Receptor Signaling	2.2
Leukocyte Extravasation Signaling	2.11
IL-10 Signaling	2.08
TREM1 Signaling	2.07
MSP-RON Signaling Pathway	2.05
Toll-like Receptor Signaling	2.01

Supplementary Figure S1. Proliferation and migration reparative ability of child hCPCs are correlated. Responses are mean-centered.

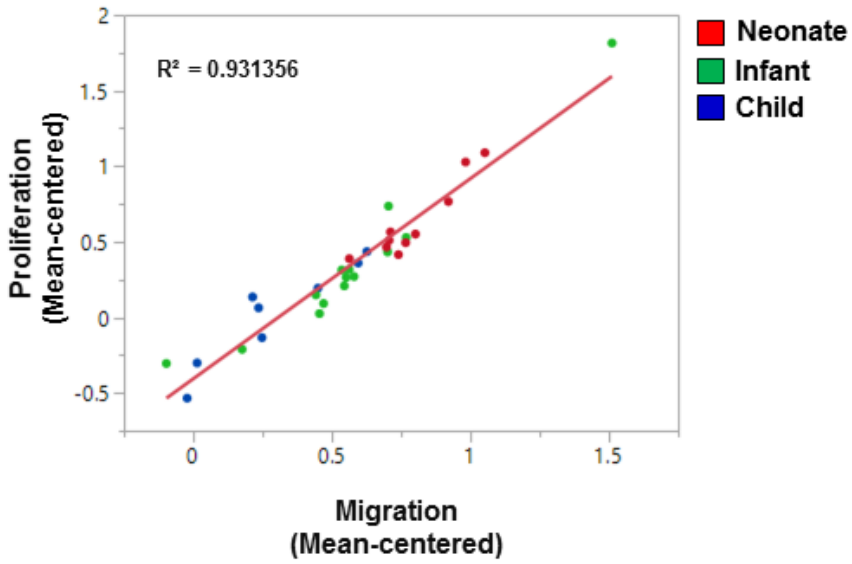

Supplementary Figure S2. Correlated genes with proliferation and migration functions. Correlation between proliferation and migration functions and the selected differentially upregulated inflammatory genes that are involved in development and growth. Signals and responses are mean-centered.

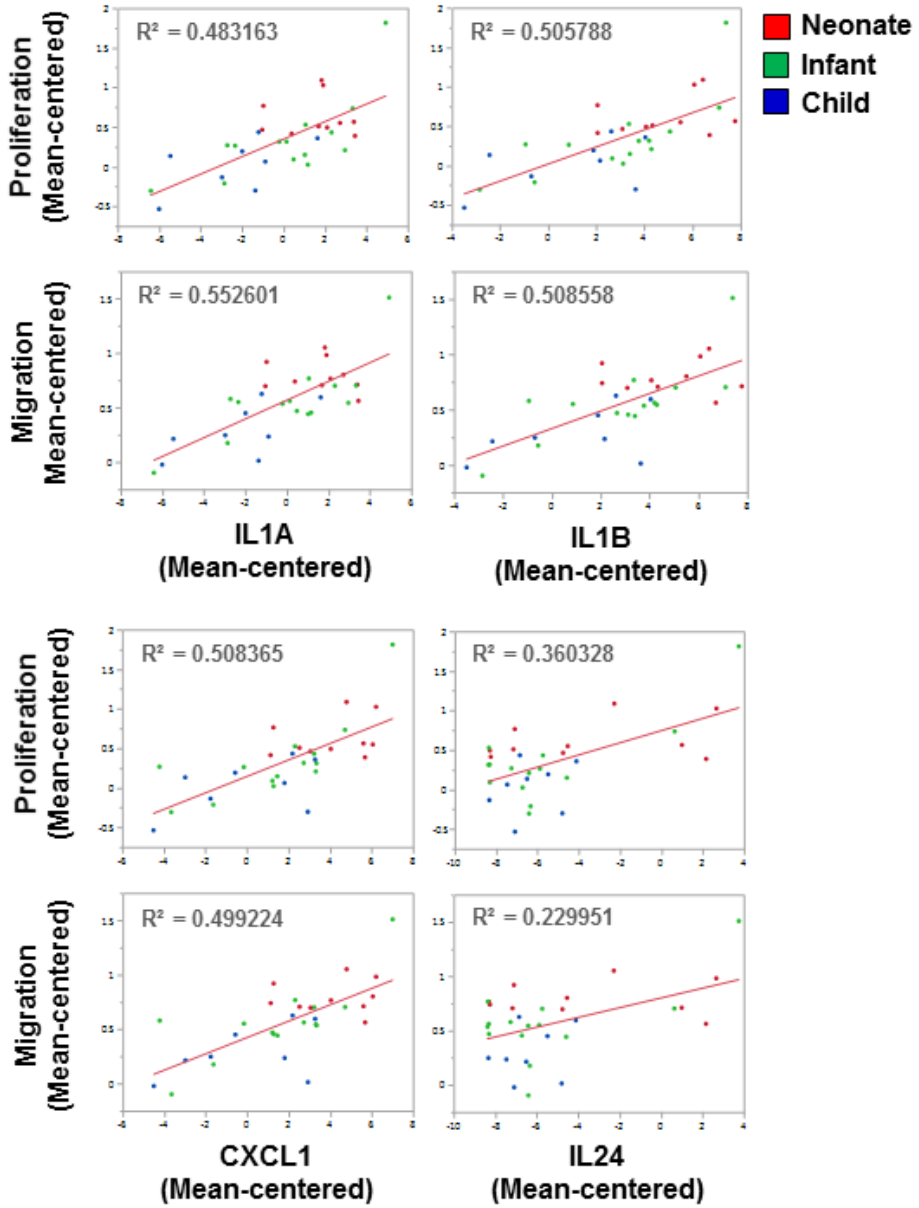

a

Supplementary Figure S3. Regression analysis of observed proliferation and migration responses with protein expression levels of CXCL6 and CXCL8 measured by ELISA in neonatal patients. Observed proliferation or migration responses for each neonate patient were plotted against CXCL6 (A,B) or CXCL8 (C) protein expression levels. Correlation between proliferation responses measured in neonatal patients did not show strong correlation with either CXCL6 or CXCL8 protein expression levels. Correlation between neonatal migration responses and CXCL6 expression level was low .